Electron Supercollimation in Graphene and Dirac Fermion Materials Using One-Dimensional Disorder Potentials

SangKook Choi,[1] Cheol-Hwan Park,[1,2] and Steven G. Louie[1,*]
[1]Department of Physics, University of California, Berkeley, California 94720, USA and Materials Sciences Division, Lawrence Berkeley National Laboratory, Berkeley, California 94720, USA
[2]Department of Physics and Center for Theoretical Physics, Seoul National University, Seoul 151-747, Korea
(Received 16 January 2014; published 9 July 2014)

Electron supercollimation, in which a wave packet is guided to move undistorted along a selected direction, is a highly desirable property that has yet to be realized experimentally. Disorder in general is expected to inhibit supercollimation. Here we report a counterintuitive phenomenon of electron supercollimation by disorder in graphene and related Dirac fermion materials. We show that one can use one-dimensional disorder potentials to control electron wave packet transport. This is distinct from known systems where an electron wave packet would be further spread by disorder and hindered in the potential fluctuating direction. The predicted phenomenon has significant implications in the understanding and applications of electron transport in Dirac fermion materials.

DOI: 10.1103/PhysRevLett.113.026802 PACS numbers: 73.22.Pr, 72.80.Ng, 72.80.Vp

Dirac fermion materials are currently one of the most intensively investigated systems in condensed matter physics and materials science [1–6]. Their conical electronic structure near the Dirac points give rise to massless neutrinolike two-dimensional electron states [7,8]. Due to the chiral nature of these Dirac fermion states, electrons interact with external potential in unusual ways, manifesting various interesting characteristics. In graphene, phenomena such as absence of backscattering by long-range potentials [9,10], Klein tunneling [11], weak antilocalization [12–15], angle-dependent electron transmission [16,17] and directional filtering of electrons due to strong angle-dependant localization exponent [18] by one-dimensional disorder in graphene superlattices, and supercollimation of electron beams by some specific one-dimensional external periodic potentials [19] have been observed or predicted. Here we present another surprising, counterintuitive electron transport phenomenon in graphene and related two-dimensional Dirac fermion systems, made possible by the carriers' unique linear dispersion relation and chiral nature. We discovered that electron supercollimation can be induced by one-dimensional disorder potentials. An electron wave packet is guided to propagate virtually undistorted along the fluctuating direction of the external one-dimensional disorder potential, independent of its initial motion, as long as the disorder is large enough to produce a wedgelike dispersion in the band structure within which the $\boldsymbol{k}$ components of the wave packet are contained. To our knowledge, this phenomenon was not known in any medium previously. Further, we find, for graphene in an external periodic potential that doesn't satisfy the supercollimation condition predicted in Ref. [19], addition of disorder would enhance collimation. The more is the disorder, the better is the supercollimation. This robust novel phenomenon has significant implications in the fundamental understanding of transport in graphene, as well as in other materials with Dirac cone physics (such as surface states of topological insulators [5] or possibly certain photonics crystals [6]), and has the potential to be exploited in the design of devices based on these materials.

We first discuss the predicted supercollimation by disorder in Dirac fermion materials using results from direct simulations (Fig. 1) and then derive the phenomenon from perturbation theory. For the low energy carriers in graphene [Fig. 2(a)] and an external potential $V(x)$ that depends only on x, we may set up an effective Hamiltonian for the electronic states [8]

$$H = \mathrm{v}_0\sigma_x p_x + \mathrm{v}_0\sigma_y p_y + V(x)I. \tag{1}$$

Here v_0 is the band velocity of the electron, σ_i is the i-component Pauli matrix, p_i is the i-direction momentum operator, and I is the identity matrix in the space describing the pseudospin components of the electron wave function. We may neglect intervalley scattering for $V(x)$ that is smooth on the interatomic scale. We carried out direct numerical simulations on the Hamiltonian in Eq. (1) using a spatially-correlated Gaussian disorder potential for $V(x)$. Such a disorder potential is characterized by a two-point correlation function having $\overline{V(x_1)V(x_2)} = \Delta^2 e^{-|x_1-x_2|/l_c}$, where Δ is the magnitude of the disorder fluctuation and l_c is the disorder correlation length. The overline represents the ensemble-averaged value. Figure 1(a) shows one realization of $V(x)$ in unit of Δ. The potential is spatially correlated so that on average it is nearly the same value within a length scale of l_c.

Figure 1(b)–(d) demonstrate supercollimation in a Gaussian wave packet propagation simulation. Using 60 different realizations of the disorder potential $V(x)$ with $l_c\Delta = 4\pi\hbar\mathrm{v}_0$,we numerically calculated the electron density $\overline{\rho(\boldsymbol{r}, t)}$ using an initial Gaussian density packet with initial

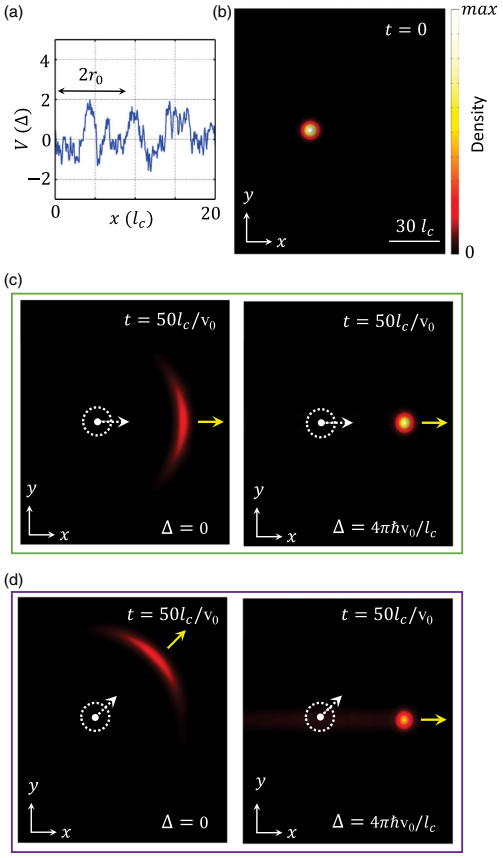

FIG. 1 (color online). (a) A realization of spatially correlated Gaussian disorder potential $V(x)$ with a magnitude Δ and correlation length l_c. (b) Initial wave packet with electron density in a Gaussian shape in coordinate space with initial center of mass wave vector $k_0 = \pi/5l_c$ and a half width of $r_0 = 5l_c$. (c)–(d) Electron density distribution in coordinate space at time $t = 50l_c/v_0$ in pristine system (left panel) and in disordered system (right panel) with initial center of mass wave vector direction (white arrow) pointing with respect to the x axis at 0° (c) and 45° (d).

center of mass wave vector $k_0 = \pi/5l_c$ and a half width of $r_0 = 5l_c$. Figure 1(c) and 1(d) show the evolution of the electron density $\rho(\boldsymbol{r}, t)$ from the initial electron density shown in Fig. 1(b). In the absence of a disorder potential, the Gaussian wave packet propagates along the initial center of mass wave vector direction marked by the white arrow and spreads sideway. Its spread angle at which the electron density is half the maximum is 48.6°. With the one-dimensional disorder potential $V(x)$, the electron package propagates nearly unspread along the potential fluctuation direction, which is x, regardless of the initial velocity direction. The spread angles are 0.5° and 0.7° at an incident angle (measured from the x axis) of 0° and 45°, respectively. A very tiny fraction of the electron density forms a supercollimated trail [barely visible in Fig. 1(d)], which increases with increasing incident angle. The same behavior is observed in simulations within a tight-binding Hamiltonian framework for graphene (see Supplemental Material [20]).

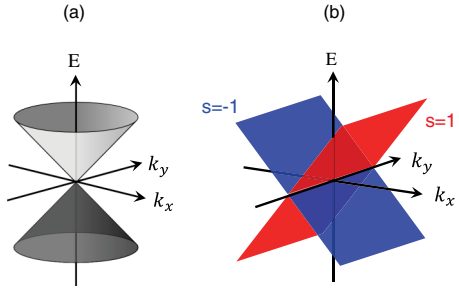

FIG. 2 (color online). (a) Low-energy electronic band structure of graphene near a Dirac point. (b) Electronic band structure of an initial two-dimensional model Hamiltonian, $H_{in} = v_0\sigma_x p_x$, where v_0 is the band velocity, σ_x is the x-component Pauli matrix and p_x is the x-direction momentum operator. This model Hamiltonian generates two chiral eigenstates which correspond to forward-moving ($s = 1$) and backward-moving ($s = -1$) states with a speed of v_0 and a pseudospin parallel to $s\hat{x}$.

We present now an analytic derivation of the phenomenon. We separate the Hamiltonian in Eq. (1) into two terms, $H = H_0 + H_1$, with $H_0 = v_0\sigma_x p_x + V(x)I$ and $H_1 = v_0\sigma_y p_y$. If H_0 dominates over H_1 (to be defined more precisely below) as in the case of an extended low-energy wave packet in real space in a disorder $V(x)$, we may regard $H_1 = v_0\sigma_y p_y$ as a perturbation.

We first show that the electron dynamics in two-dimension governed by $H_0 = v_0\sigma_x p_x + V(x)I$ alone yields supercollimation along the direction. The term $v_0\sigma_x p_x$ has two eigenstates ($s = \pm 1$) as shown in Fig. 2(b). By a unitary transformation of $U = \frac{1}{\sqrt{2}}\begin{pmatrix} 1 & 1 \\ 1 & -1 \end{pmatrix}$, $U^\dagger v_0 p_x \sigma_x U$ is diagonal with eigenvalues $s\hbar v_0 k_x$ with $s = \pm 1$, and eigenvectors $\frac{1}{\sqrt{A}}\begin{pmatrix} e^{ik\cdot r} \\ 0 \end{pmatrix}'$ and $\frac{1}{\sqrt{A}}\begin{pmatrix} 0 \\ e^{ik\cdot r} \end{pmatrix}'$, respectively, where A is the area of the sample and the prime notation here indicates a matrix or vector in the unitary-transformed or pseudospin basis. These are chiral states moving forward ($s = 1$) or backward ($s = -1$) with a speed of v_0 and a pseudospin aligned along the propagation direction. The retarded Green's function G_0' of $H_0' = U^\dagger H_0 U$ in coordinate space is given by

$$G_0'(\boldsymbol{r},\boldsymbol{r}',t) = \frac{1}{i\hbar}\theta(t)\delta(y-y') \times \begin{pmatrix} \delta(x-x'-v_0t)\alpha(x,x') & 0 \\ 0 & \delta(x'-x-v_0t)\alpha(x',x) \end{pmatrix} \quad (2)$$

with

$$\alpha(x,x') = \exp\left(\frac{1}{i\hbar v_0}\int_{x'}^{x} V(x_1)dx_1\right) \quad (3)$$

(see Supplemental Material [20] for the derivation of Eq. (2); G_0' is consistent with the transfer matrix in Ref. [21].) The Green's function determines the time evolution of the electron wave function and density through

$$\psi'(\boldsymbol{r},t)=\int d\boldsymbol{r}'i\hbar G'(\boldsymbol{r},\boldsymbol{r}',t)\psi'_0(\boldsymbol{r}',t=0), \tag{4}$$

and

$$\rho(\boldsymbol{r},t)=tr[\psi'(\boldsymbol{r},t)\psi'^{\dagger}(\boldsymbol{r},t)], \tag{5}$$

where the trace is defined with respect to the 2×2 pseudospin subspace. (We recall that $\psi'(\boldsymbol{r},t)$ is a two-component spinor function and the total density $\rho(\boldsymbol{r},t)$ is a sum over densities from the two components.) As seen from the diagonal-matrix form of $G'_0(\boldsymbol{r},\boldsymbol{r}',t)$ in Eq. (2), scattering between two states with different chirality (or group velocity) is not allowed for any arbitrary external potential $V(x)$, if we neglect H_1. Consequently, for the Hamiltonian H'_0, the amplitude of any initial wave function $\psi'(\boldsymbol{r},t=0)$ with pseudospin s moves at a velocity of $s\mathrm{v}_0$, maintaining its initial shape, although the phase of the wave function is changed by the interaction with the potential $V(x)I$. The electron density of a wave packet with a pseudospin s thus also propagates with a velocity of $s\mathrm{v}_0$ along the x direction, maintaining its original shape at $t=0$, again, if H'_1 is neglected. To illustrate this point, if we take an initial Gaussian wave packet with initial center of mass wave vector $\boldsymbol{k}_0$ and a half width of $\sqrt{2}r_0$,

$$\psi'(\boldsymbol{r},t=0)=\frac{1}{\sqrt{2\pi}r_0}\begin{pmatrix}1\\0\end{pmatrix}'\exp\left(-\frac{r^2}{4r_0^2}+i\boldsymbol{k}_0\cdot\boldsymbol{r}\right), \tag{6}$$

then, as a function of time, the electron density is given by (from Eqs. (4) and (5))

$$\rho^{(0)}(\boldsymbol{r},t)=\frac{1}{2\pi r_0^2}\exp\left(-\frac{|\boldsymbol{r}-\mathrm{v}_0t\hat{\boldsymbol{x}}|^2}{2r_0^2}\right). \tag{7}$$

The disorder potential $V(x)$ generates a random phase accumulation for the electron which may be loosely thought of as an effective elastic mean free path l_s or elastic collision time τ for electrons governed by H'_0. The quantity l_s may be extracted from $\bar{G}'_0$. In the expression for G'_0 given by Eq. (2), the quantity $\alpha(x,x')$ incorporate all the effects of $V(x)$. For a random potential, translation symmetry is restored by ensemble average [22], so that $\overline{\alpha(x,x')}=\overline{\alpha(x-x')}$. The form of α in Eq. (3) dictates that $\overline{\alpha(x-x')}$ has its maximum at $x=x'$, and decreases as $|x-x'|$ increases since the phase of $\alpha(x,x')$ fluctuates from one member to another in an ensemble. If we assume that $\overline{\alpha(x,x')}$ decays with a full width at half maximum of l_s, then $\overline{G'_0(\boldsymbol{r}-\boldsymbol{r}',t)}$ decays with the same mean-distance l_s. The effective elastic collision time τ is obtained by considering $\bar{G}'_0$ in Fourier space. A Fourier transform of Eq. (2) yields

$$\overline{G'_0(\boldsymbol{k},\omega)}=\int dE'\frac{1}{\hbar\omega-E'+i\eta}\times\begin{pmatrix}A_0(E'-\hbar\mathrm{v}_0k_x)&0\\0&A_0(E'+\hbar\mathrm{v}_0k_x)\end{pmatrix} \tag{8}$$

with

$$A_0(E)=\frac{1}{2\pi\hbar\mathrm{v}_0}\int dx\,\overline{\alpha(x)}\exp\left(i\frac{E}{\hbar\mathrm{v}_0}x\right). \tag{9}$$

The function $A_0(E'-s\hbar\mathrm{v}_0k_x)$ here plays the role of the spectral function $A_0(s,\boldsymbol{k},\omega)$. Due to the decay of $\overline{\alpha(x)}$, $A_0(s,\boldsymbol{k},\omega)$ is maximum at $\omega=s\mathrm{v}_0k_x$ and has a finite width, owing to the finite effective elastic collision time, which is independent of the momentum $\boldsymbol{k}$. From the full width at half maximum of $A_0(s,\boldsymbol{k},\omega)$, we can deduce τ. For example, for a spatially correlated Gaussian disorder, one obtains

$$\overline{\alpha(x)}=\exp\left[-\left(\frac{l_c\Delta}{\hbar v_0}\right)^2\left\{\exp\left(-\frac{|x|}{l_c}\right)-1+\frac{|x|}{l_c}\right\}\right]. \tag{10}$$

Let us now consider the effects of $H_1=\mathrm{v}_0\sigma_yp_y$ and show that electron supercollimation still persists over a large distance L_0. We show this by examining the time evolution of the electron density $\rho(\boldsymbol{r},t)$ by the full Hamiltonian $H'=U^{\dagger}HU$ from a series expansion of the wave function up through third order in $H'_1=U^{\dagger}H_1U=-v_0p_y\sigma_y$, i.e., $\psi'(\boldsymbol{r},t)\approx\sum_{i=0}^{3}\psi'^{(i)}(\boldsymbol{r},t)$, where the change in the wave function in ith order is given by $\psi'^{(i)}(\boldsymbol{r},t)$. Then, $\rho(\boldsymbol{r},t)\approx\sum_{i=0}^{3}\rho^{(i)}(\boldsymbol{r},t)$ with $\rho^{(i)}(\boldsymbol{r},t)\equiv\sum_{\substack{j,k=0\\j+k=i}}^{3}\rho^{(i)}_{jk}(\boldsymbol{r},t)$ and $\rho^{(j+k)}_{jk}(\boldsymbol{r},t)=\mathrm{tr}[\psi'^{(j)}(\boldsymbol{r},t)\psi'^{(k)\dagger}(\boldsymbol{r},t)]$. The zeroth-order term $\rho^{(0)}$, given by Eq. (7), is already shown to be a collimated electron density with unchanging shape. Up to the third order in H'_1, it is straightforward to show that all terms in the above expression for $\rho(\boldsymbol{r},t)$, except one, retain the initial extent of the wave packet and move along the x direction with the same velocity. Only the $\rho^{(2)}_{11}(\boldsymbol{r},t)$ term shows shape deviation, but it still does not spread along the y direction and is collimated to move along the x direction (for the details, see Supplemental Material [20]). To illustrate this, for $r_0>l_s$ and with an initial wave packet given by Eq. (6), $\bar{\rho}^{(2)}_{11}(\boldsymbol{r},t)$ is

$$\bar{\rho}^{(2)}_{11}(\boldsymbol{r},t)\approx\frac{l_s}{2\sqrt{2\pi}r_0}\left(k_{0y}^2+\frac{y^2}{4r_0^4}\right)e^{-y^2/2r_0^2}\left(-\mathrm{Erf}\left(\frac{x-v_0t}{\sqrt{2}r_0}\right)+\mathrm{Erf}\left(\frac{x+v_0t}{\sqrt{2}r_0}\right)\right). \tag{11}$$

This corresponds to a strip of density of width $2r_0$ determined by the initial wave packet but extended from v_0t to $-v_0t$ in the $\hat{x}$ direction. If we compare $\int d\boldsymbol{r}\overline{\rho^{(2)}_{11}(\boldsymbol{r},t)}$ with $\int d\boldsymbol{r}\rho^{(0)}(\boldsymbol{r},t)$, $\int d\boldsymbol{r}\overline{\rho^{(2)}_{11}(\boldsymbol{r},t)}<\int d\boldsymbol{r}\rho^{(0)}(\boldsymbol{r},t)$ for $(2k_{0y}^2+1/(2r_0^2))l_s\mathrm{v}_0t<1$, giving rise to supercollimation with little diminishment of the intensity of the original Gaussian profile over a distance of roughly $L_0=v_0t=1/(2l_sk_{0y}^2+l_s/(2r_0^2))$. For example, for a disorder potential that gives a broadening of 0.2 eV in the spectral function,

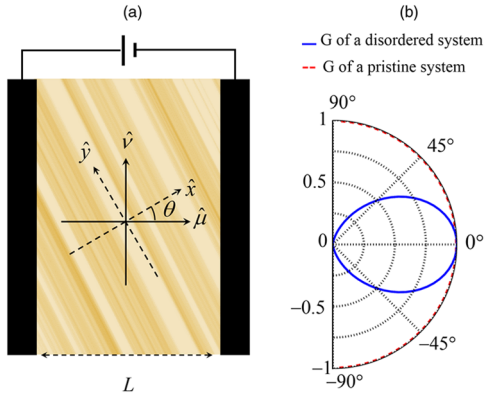

FIG. 3 (color online). (a) Schematic diagram of experimental setup for proposed conductance measurement. Two electrodes are in contact with graphene under one-dimensional disorder potential fluctuating along the $\hat{x}$ direction. The electrodes are separated by a distance L along the $\hat{\mu}$ direction. (b) Calculated conductance $G(L,\theta)$ (in a unit of $2N_\nu e^2/h$ where N_ν is the number of subbands due to the confinement along the ν direction at energy E_F) as a function of the angle θ in a pristine system in the ballistic regime (red line) and in a system with one-dimensional disorder potential ($l_s \ll L$) shown in (a) from Eq. (14) (blue line).

a wave packet with $r_0 > 40$ nm $\approx 250a_{cc}$ and a center of mass wave vector such that $\hbar v_0 k_{0y} < 0.01$ eV will undergo supercollimation for nearly a micrometer.

We propose a possible experiment to demonstrate the predicted electron supercollimation phenomenon by measuring the conductance G in a geometry shown in Fig. 3(a). In this set up, graphene or a Dirac fermion material is in contact with two electrodes that are separated at a distance L along the $\hat{\mu}$ direction. This direction is at an angle θ with respect to the one-dimensional potential fluctuation direction $\hat{x}$. The conductance G between the two electrodes is, according to the Kubo formula [23,24],

$$G(L,\theta) = \int d\boldsymbol{r}d\boldsymbol{r}'\sigma_{\mu\mu}(\boldsymbol{r},\boldsymbol{r}',E_F)\delta(\mu)\delta(\mu'-L), \qquad (12)$$

with conductivity

$$\sigma_{\mu\mu}(\boldsymbol{r},\boldsymbol{r}',E_F) = \frac{\pi\hbar}{(2\pi i)^2}\mathrm{tr}\Big[j_\mu(\boldsymbol{r})(G^{R-A}(\boldsymbol{r},\boldsymbol{r}',E_F)) \times j_\mu(\boldsymbol{r}')(G^{R-A}(\boldsymbol{r}',\boldsymbol{r},E_F))\Big], \qquad (13)$$

where $\boldsymbol{j} = e\mathrm{v}_0\boldsymbol{\sigma}$ [25]. The quantity G^{R-A} is defined as $G^{R-A} = G^R - G^A$ with G^R and G^A being the retarded and advanced Green's functions, respectively. If we expand the ensemble-averaged conductance $\overline{G(L,\theta)}$ up to and including the first-order term in H_1 (see Supplemental Material [20]),

$$\overline{G(L,\theta)} \propto \cos^2\theta + \sin^2\theta\exp[-2L/(l_s\cos\theta)] \times \cos(2E_FL/(\hbar\mathrm{v}_0\cos\theta)) \qquad (14)$$

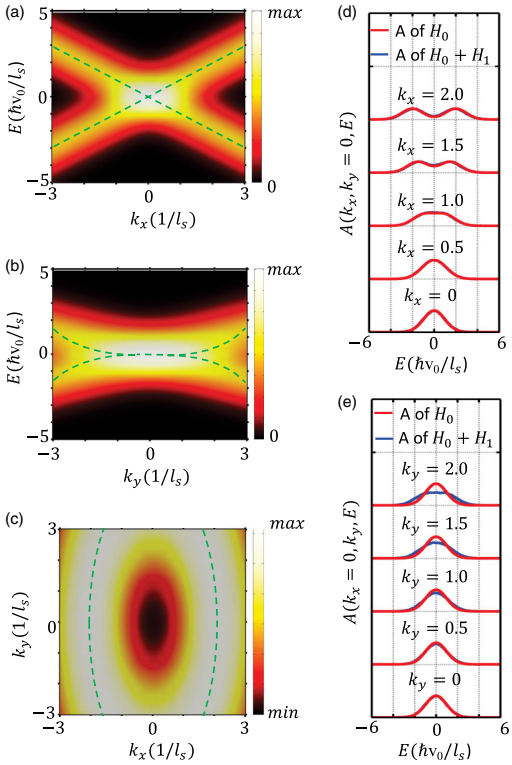

FIG. 4 (color online). (a)–(c) Numerically evaluated spectral function, $A(\boldsymbol{k},E) = -\mathrm{trIm}\overline{G'(\boldsymbol{k},E)}/\pi$, for $l_c\Delta = 4\pi\hbar\mathrm{v}_0$ along the $k_y = 0$ line (a), along the $k_x = 0$ line (b), and on the $E = 2\hbar\mathrm{v}_0/l_s$ plane with $l_s = \hbar\mathrm{v}_0/\Delta$ (c). (d)–(e) The line shapes of the spectral function of $H_0 = \mathrm{v}_0\sigma_x p_x + V(x)I$ (red lines) and of $H_0 + H_1$ (blue lines) with $H_1 = \mathrm{v}_0\sigma_y p_y$ at various k_x with $k_y = 0$ (d), and at various k_y with $k_x = 0$ (e).

This is dramatically distinct from that of a gated pristine graphene in the ballistic regime, in which case the conductance $G(L,\theta)$ is constant regardless of the orientation angle θ.

The ensemble-average dispersion relation of the electrons in graphene is strongly and anisotropically renormalized in the presence of the random potential $V(x)$ for $|k_y| < 1/l_s$ (for details, see Supplemental Material [20]), forming a wedgelike structure for the energy surface $E(\boldsymbol{k})$. We demonstrate this effect by calculating the ensemble-average spectral function. Using 60 different realizations of the disorder with $l_c\Delta = 4\pi\hbar\mathrm{v}_0$, we numerically calculated $\mathrm{Im}G'(\boldsymbol{k},\omega)$. Figure 4 shows the 60-ensemble-average spectral function, $A(\boldsymbol{k},E) = -\mathrm{trIm}\overline{G'(\boldsymbol{k},E)}/\pi$ where the trace is with respect to the 2×2 pseudospin subspace. Along the $\boldsymbol{k} = (k_x, 0)$ line, shown in Fig. 4(a), the dispersion relation is linear and it follows the $E = \pm\hbar\mathrm{v}_0 k_x$ lines, which is the dispersion relation of the pristine system. However, along the $\boldsymbol{k} = (0, k_y)$ line, shown in Fig. 4(b), the band structure is strongly renormalized near the Dirac point and becomes flat. The anisotropic renormalization of the band structure can be demonstrated more clearly by a contour plot of $A(\boldsymbol{k},E)$ on the k_x-k_y plane with $E = 2\hbar v_0/l_s$, as shown in Fig. 4(c). On this constant energy plane, constant amplitude

lines of $A(\boldsymbol{k}, E)$ are oval shaped and stretched along the k_y direction. For spatially correlated Gaussian disorder potentials, we can evaluate explicitly the spectral function of $\bar{G}'_0$ from the Fourier transform of Eq. (10). For this particular kind of disorder, the line shape of the spectral function at different k_x with $|k_{0y}| < 1/l_s$ is identical and $\tau \sim \hbar/\Delta$ (if $l_c > \hbar v_0/\Delta$). As shown in Fig. 4(d), the line shape from Eqs. (9) and (10) matches well with numerically simulated line shape from $\bar{G}'$ at various k_x with $k_y = 0$. However, as k_y increases (at $k_x = 0$), the numerically calculated spectral function deviates from the line shape from $\overline{\alpha(x)}$ owing to the effect of H'_1.

Electron beam supercollimation has been predicted theoretically in certain special graphene superlattices (SGS): a graphene sheet modulated by a one-dimensional periodic potential satisfying certain specific conditions [19]. In the experimental realization of such SGS (e.g., using substrate [26], controlled adatom deposition [27], ripples [28] under perpendicular electric field [29,30], or gating [31]), it would be unavoidable to have some disorders in the external potential, which previously thought might impede the supercollimation effect. However, we found in this study that one-dimensional disorder along the periodic potential modulation direction in fact enhances supercollimation for an external periodic potential, with such enhancement occurring even if the external potential does not exactly satisfy the SGS supercollimation condition. For a detailed discussion and numerical simulation of this phenomenon, please see Supplemental Material [20].

In summary, through perturbation theory analysis and numerical simulations, we have discovered a highly counterintuitive phenomenon of electron supercollimation via one-dimensional disorder potential in graphene and other Dirac fermion materials. To our knowledge, this phenomenon is not seen in any other systems.

We wish to thank M. L. Cohen and G. Y. Cho for discussions. Analytical calculations were supported by National Science Foundation Grant No. DMR10-1006184. Numerical calculation was supported by the Theory Program at the Lawrence Berkeley National Lab funded by the Director, Office of Science, Office of Basic Energy Sciences, Materials Sciences and Engineering Division, U.S. Department of Energy under Contract No. DE-AC02-05CH11231. Computational resources have been provided by the DOE at Lawrence Berkeley National Laboratory's NERSC facility. S. G. L. acknowledges support by a Simons Foundation Fellowship in Theoretical Physics and C. -H. P. by Korean NRF funded by MSIP (Grant No. NRF-2013R1A1A1076141).

*sglouie@berkeley.edu

[1] K. S. Novoselov, A. K. Geim, S. V. Morozov, D. Jiang, Y. Zhang, S. V. Dubonos, I. V. Grigorieva, and A. A. Firsov, Science **306**, 666 (2004).
[2] K. S. Novoselov, D. Jiang, F. Schedin, T. J. Booth, V. V. Khotkevich, S. V. Morozov, and A. K. Geim, Proc. Natl. Acad. Sci. U. S. A. **102**, 10451 (2005).
[3] K. S. Novoselov, A. K. Geim, S. V. Morozov, D. Jiang, M. I. Katsnelson, I. V. Grigorieva, S. V. Dubonos, and A. A. Firsov, Nature (London) **438**, 197 (2005).
[4] Y. Zhang, Y.-W. Tan, H. L. Stormer, and P. Kim, Nature (London) **438**, 201 (2005).
[5] M. Z. Hasan and C. L. Kane, Rev. Mod. Phys. **82**, 3045 (2010).
[6] X. Huang, Y. Lai, Z. H. Hang, H. Zheng, and C. T. Chan, Nat. Mater. **10**, 582 (2011).
[7] P. R. Wallace, Phys. Rev. **71**, 622 (1947).
[8] G. W. Semenoff, Phys. Rev. Lett. **53**, 2449 (1984).
[9] T. Ando and T. Nakanishi, J. Phys. Soc. Jpn. **67**, 1704 (1998).
[10] P. L. McEuen, M. Bockrath, D. H. Cobden, Y.-G. Yoon, and S. G. Louie, Phys. Rev. Lett. **83**, 5098 (1999).
[11] M. I. Katsnelson, K. S. Novoselov, and A. K. Geim, Nat. Phys. **2**, 620 (2006).
[12] J. H. Bardarson, J. Tworzydło, P. W. Brouwer, and C. W. J. Beenakker, Phys. Rev. Lett. **99**, 106801 (2007).
[13] K. Nomura, M. Koshino, and S. Ryu, Phys. Rev. Lett. **99**, 146806 (2007).
[14] P. San-Jose, E. Prada, and D. S. Golubev, Phys. Rev. B **76**, 195445 (2007).
[15] M. Titov, Europhys. Lett. **79**, 17004 (2007).
[16] Y. P. Bliokh, V. Freilikher, S. Savel'ev, and F. Nori, Phys. Rev. B **79**, 075123 (2009).
[17] N. Abedpour, A. Esmailpour, R. Asgari, and M. R. R. Tabar, Phys. Rev. B **79**, 165412 (2009).
[18] Q. Zhao, J. Gong, and C. A. Müller, Phys. Rev. B **85**, 104201 (2012).
[19] C.-H. Park, Y.-W. Son, L. Yang, M. L. Cohen, and S. G. Louie, Nano Lett. **8**, 2920 (2008).
[20] See Supplemental Material at http://link.aps.org/supplemental/10.1103/PhysRevLett.113.026802 for additional analytical and numerical results.
[21] V. V. Cheianov and V. I. Fal'ko, Phys. Rev. B **74**, 041403 (2006).
[22] P. Sheng, *Introduction to Wave Scattering: Localization and Mesoscopic Phenomena* (Springer, New York, 2006).
[23] D. S. Fisher and P. A. Lee, Phys. Rev. B **23**, 6851 (1981).
[24] É. Akkermans and G. Montambaux, *Mesoscopic Physics of Electrons and Photons* (Cambridge University Press, Cambridge, England, 2007).
[25] S. Ryu, C. Mudry, A. Furusaki, and A. W. W. Ludwig, Phys. Rev. B **75**, 205344 (2007).
[26] S. Marchini, S. Günther, and J. Wintterlin, Phys. Rev. B **76**, 075429 (2007).
[27] J. C. Meyer, C. O. Girit, M. F. Crommie, and A. Zettl, Appl. Phys. Lett. **92**, 123110 (2008).
[28] W. Bao, F. Miao, Z. Chen, H. Zhang, W. Jang, C. Dames, and C. N. Lau, Nat. Nanotechnol. **4**, 562 (2009).
[29] L. Brey and J. J. Palacios, Phys. Rev. B **77**, 041403 (2008).
[30] A. Isacsson, L. M. Jonsson, J. M. Kinaret, and M. Jonson, Phys. Rev. B **77**, 035423 (2008).
[31] S. Dubey, V. Singh, A. K. Bhat, P. Parikh, S. Grover, R. Sensarma, V. Tripathi, K. Sengupta, and M. M. Deshmukh, Nano Lett. **13**, 3990 (2013).